CHAPTER 2

THEORETICAL BACKGROUND

2.1. Basic Concepts of Spectroscopy

Spectroscopy is a scientific discipline concerned with the interactions of electromagnetic radiation with matter [2]. When the electromagnetic radiation impinges on the surface of an object, interactions between the incident beam and the molecules will alter the incident radiation. The incident beam can be reflected, scattered, transmitted, or absorbed by the matter. Since a spectroscopic experiment allows detection of reflected, scattered, transmitted, or absorbed light, it needs a source of light or excitation, an object of study, and a suitable detector. Thus, changes in the electromagnetic radiation can be observed. The modification of the electromagnetic radiation by the matter carries information about the molecular information or physical properties of the matter.

While an object and a detector are defined by specific chemical and physical properties, light needs further consideration. Light is an electromagnetic wave. In its simplest monochromatic form, light can be represented as oscillating electric and magnetic fields that propagate in space [2] (see Figure 2.1). The electric and magnetic vectorial components are orthogonal to each other and to the direction of propagation.

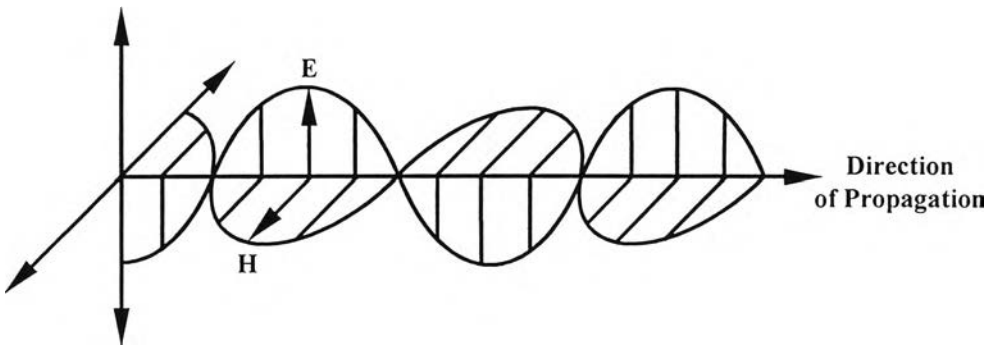

Figure 2.1 Propagation of a linearly polarized electromagnetic wave in the direction of propagation.

When such an electromagnetic radiation impinges on a specimen, rays of the incident beam may be reflected, scattered, transmitted, or absorbed. Depending on the experimental arrangement. The total amount of incident energy is the sum of reflected, scattered, transmitted, and absorbed light. A schematic illustration for an interaction between light and matter is illustrated in Figure 2.2. This process can be expressed by the following relationship [2]:

$$I_0 = I_R + I_S + I_T + I_A \tag{2.1}$$

where I_0 is the intensity of the incident beam and I_R, I_S, I_T, and I_A are the reflected, scattered, transmitted, and absorbed beams, respectively. The intensity of each beam depends on the intensity and wavelength of the incident radiation, the optical properties of the specimen, the concentrations of species, and the geometry of the experimental setup.

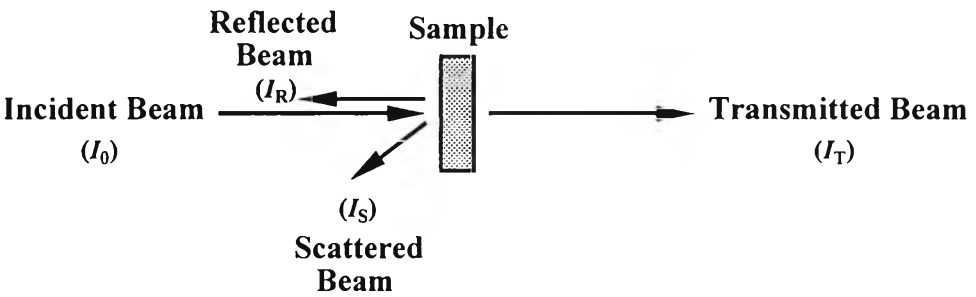

Figure 2.2 Interactions of light with matter.

Let's consider the electromagnetic radiation when a sample is inserted between a source of light and a detector. The sample absorbs a fraction of the incident radiation. In order to measure the region and amount of light being absorbed by the sample, we need to measure the ratio of the sample attenuated (I) and nonattenuated (I_0) intensities of the radiation. The ratio is proportional to the transmittance of the sample. This relationship can be quantitatively related to the chemical composition of the sample by the Beer-Lambert law as [2]:

$$I / I_0 = e^{-A(\bar{\nu})} = e^{-c_2 \varepsilon(\bar{\nu}) l} \tag{2.2}$$

where $A(\bar{\nu})$ is the sample absorbance at a given wavenumber $\bar{\nu}$, c_2 is the concentration of the absorbing functional group, $\varepsilon(\bar{\nu})$ is the wavenumber-dependent absorption coefficient, and l is the film thickness for the IR beam at a normal incidence to the sample surface.

A simple transmission experiment as described above may provide a significant amount of information concerning molecular structures and their properties. One apparent drawback is that the technique is not applicable to surface analysis. If one want to gain an insight understanding of the surface properties such as chemical compositions, molecular orientation, and chemical reaction, a surface sensitive technique is required. ATR FT-IR is a good candidate for that purpose. It is not only a technique that provides the information, which directly associated to chemical composition of the sample but also a surface sensitive sensitive technique.

2.2. ATR FT-IR Spectroscopy

2.2.1. Introduction

ATR FT-IR spectroscopy stand for attenuated total reflection Fourier transform infrared spectroscopy. It is a material characterization technique using an internal reflection principle. The total internal reflection is an optical phenomenon, which can be observed easily, for example, with a glass of water. If the side of the glass below the water level is viewed obliquely through the water surface, it appears to be completely silvered and one can no longer see objects behind it. The reason for this is that light striking the glass surface is totally reflected and therefore does not pass through the surface to illuminate these objects.

The unusual characteristics associated with total internal reflection can be utilized with advantage in many areas. These applications include precision measurements of angles and refractive indices; the construction of beam splitters, optical filters, laser cavities, light modulators, light deflectors; and the measurement of film thickness and surface relief.

2.2.2. Principles of Light Reflection and Refraction

When electromagnetic radiation strikes an interface between two media with different refractive indices, refraction and reflection occurs. The law that governs the reflection process requires that the angle of incidence be equal to the angle of reflection. In this case, reflection is specular. If electromagnetic radiation passes from one medium to another that has a different refractive index, a sudden change of beam direction is detected because of the difference in propagation velocity through two media. If light propagates through a medium with refractive index n_1 and enters a medium with refractive index n_2 (see Figure 2.3), the light path will change, the extent of refraction is given by the following relationship [2]:

$$\frac{\sin \alpha_1}{\sin \alpha_2} = \frac{n_2(\bar{\nu})}{n_1(\bar{\nu})} \tag{2.3}$$

where α_1 and α_2 are the angle of incidence and the angle of refraction, respectively.

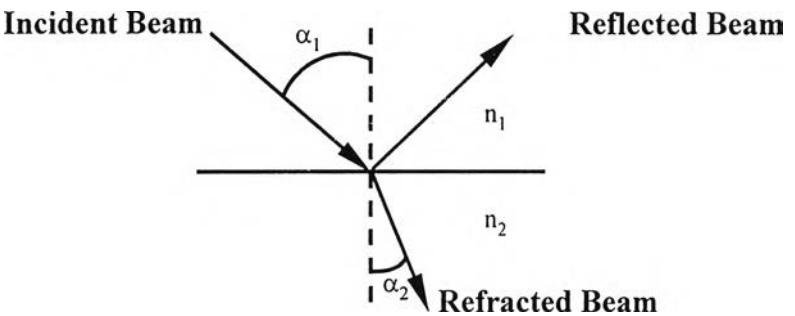

Figure 2.3 Snell's Law.

Total internal reflection occurs when light traveling in an optically denser medium impinges on surface of a rarer medium (i.e., $n_1 > n_2$) with an incident angle greater than the critical angle. The critical angle can be derived from snell's law and given by Equation 2.4 [2, 3]. According to Figure 2.4, when the angle of incidence equals the critical angle, θ_c , the refracted angle equals 90°. This implies that under a total internal reflection phenomenon there is no light from the optically denser medium travels across the interface into the optically rarer medium.

$$\theta_c = \sin^{-1}(n_2(\bar{\nu}) / n_1(\bar{\nu})). \tag{2.4}$$

Total Internal reflection spectroscopy is, therefore, the technique of recording the optical spectrum of a sample material that is in contact with an optically denser medium. The wavelength dependence of the reflectivity of this interface is measured by introducing light into the denser medium, as shown in Figure 2.4. In this technique the reflectivity is a measure of the interaction of the electric field with the material and the resulting spectrum is also a characteristic of the material. Since the technique complements conventional optical absorption

techniques and can be used in some instances where conventional technique cannot readily be applied, the areas of application of optical spectroscopy are, thus, extended.

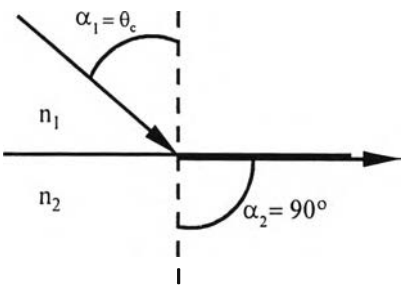

Figure 2.4 Conditions under which total internal reflection occurs. Light travels from an optically denser medium and impinges at the surface of the optically rarer medium ($n_1 > n_2$).

2.2.3. Internal Reflection Elements (IRE)

The internal reflection element (IRE) is an infrared transparent material used in internal reflection spectroscopy for establishing the conditions necessary to obtain internal reflection spectra of materials (see Figure 2.5). Radiation propagates through the IRE by means of internal reflection. The sample material is placed into contact with the IRE. The ease of obtaining an internal reflection spectrum and the information obtained from the spectrum are determined by a number of characteristics of the IRE. A choice must be made in the working angle or range of angles of incidence, number of reflections, aperture, number of passes, surface preparation, and material from which it is made [3].

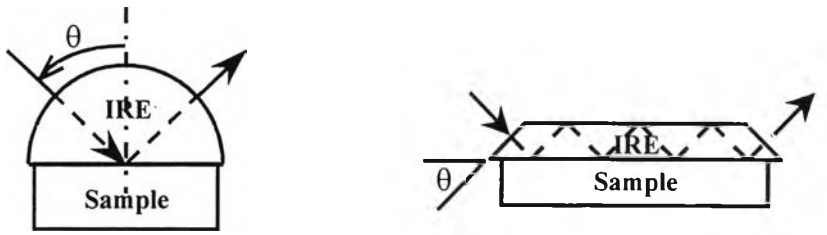

a.) Single Reflection **b.) Multiple Reflection**

Figure 2.5 Selected IRE configurations commonly used in ATR experimental setups: a.) Single reflection variable-angle hemispherical or hemicylinder crystal, and b.) Multiple reflection single-pass crystal.

2.2.4. ATR Spectral Intensity

If there is no other cause for energy loss beside absorption by the sample is assumed, the following expression is obtained for ATR spectral intensity [4]:

$$A(\theta, \nu) = 1 - R(\theta, \nu) \tag{2.5}$$

where $A(\theta, \nu)$ is absorptance and $R(\theta, \nu)$ is reflectance. Absorptance in ATR can be expressed in terms of experimental parameters and material characteristics by the following expression [2]:

$$A_{\bar{p}}(\theta, \nu) = \frac{4\pi\nu}{n_0 \cos\theta} \int_0^{\infty} n_1(\nu) k_1(\nu) \left\langle E_z^2(\theta, \nu) \right\rangle dz \tag{2.6}$$

where $\bar{p}$ indicates degree of polarization of the incident beam, $\left\langle E_z^2(\theta, \nu) \right\rangle$ is the mean square electric field (MSEF) at depth z, $n_1(\nu)$ and $k_1(\nu)$, respectively, are the refractive index and absorption index of the sample, and n_0 is the refractive index of the IRE. The MSEF is strongest at the IRE/sample interface. Its strength

decreases exponentially as a function of depth. The MSEF is, however, also a function of experimental condition and material characteristics.

The MSEF at various conditions are shown in Figure 2.6.

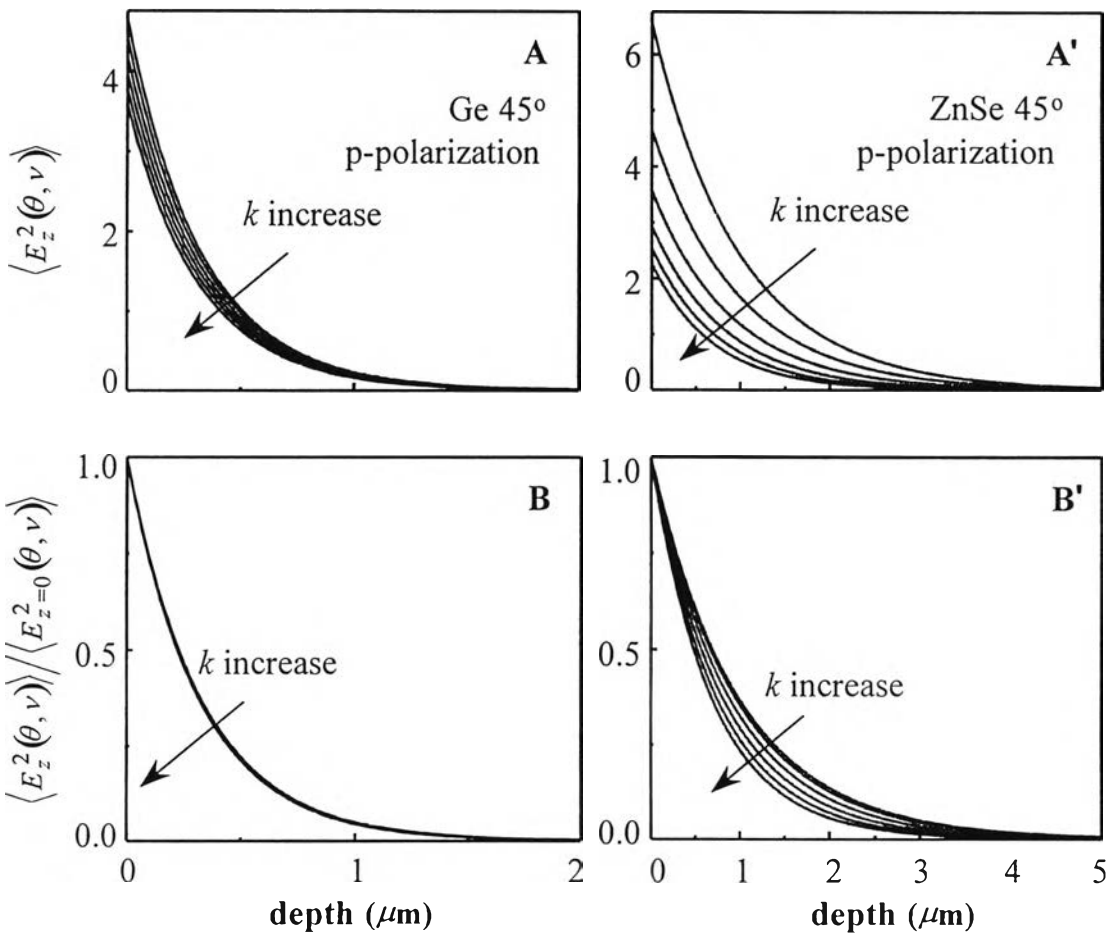

Figure 2.6 The MSEF at various experimental condition (A, A′) and its decay characteristic (B, B′). The simulation parameters are $n_0 = 4.00$ for Ge, $n_0 = 2.40$ for ZnSe, $\nu = 1000\ cm^{-1}$, $n_1(\nu) = 1.50$, $k_1(\nu) = 0.0, 0.1, 0.2, 0.3, 0.4$, and 0.5, respectively.

Figure 2.6 indicates that the strength and decay characteristic of the MSEF vary with the absorption strength. Under an experimental condition, absorption increases with the absorption index $k_1(\nu)$. In fact, if one wants to calculate the

MSEF, the complex refractive index of the material (i.e., the refractive index and the absorption index) must be known. Under a non-absorbing condition (i.e., $k_1(\nu) = 0$). The MSEF can be calculated if the refractive index of material is known. Under this condition, the MSEF is given a special name as the mean square evanescent field (MSEvF). The strength and decay characteristic of the MSEvF can be given in a much simpler expression. The MSEvF at the interface with p- and s-polarized radiation is given, respectively, by [3]:

$$\left\langle E^2_{p,z=0}(\theta,\nu)\right\rangle_{k=0} = \frac{4\cos^2\theta\left|\sin^2\theta - (n_1(\nu)/n_0)^2\right| + 4\cos^2\theta\sin^2\theta}{\left[1-(n_1(\nu)/n_0)^2\right]\left\{\left[1+(n_1(\nu)/n_0)^2\right]\sin^2\theta - (n_1(\nu)/n_0)^2\right\}} \quad (2.7)$$

$$\left\langle E^2_{s,z=0}(\theta,\nu)\right\rangle_{k=0} = \frac{4\cos^2\theta}{1-(n_1(\nu)/n_0)^2} \quad (2.8)$$

The decay characteristic of the MSEvF is given in terms of the penetration depth by:

$$\left\langle E^2_z(\theta,\nu)\right\rangle = \left\langle E^2_0(\theta,\nu)\right\rangle e^{-2z/d_p(\theta,\nu)} \quad (2.9)$$

$$d_p = \frac{1}{2\pi\nu n_0(\sin^2\theta - (n_1/n_0)^2)^{1/2}} \quad (2.10)$$

where $d_p(\theta,\nu)$ is the penetration depth. The penetration depth also depends on experimental conditions and material characteristics. Example of the penetration depth at various experimental conditions and material characteristics are shown in Figures 2.7 and 2.8.

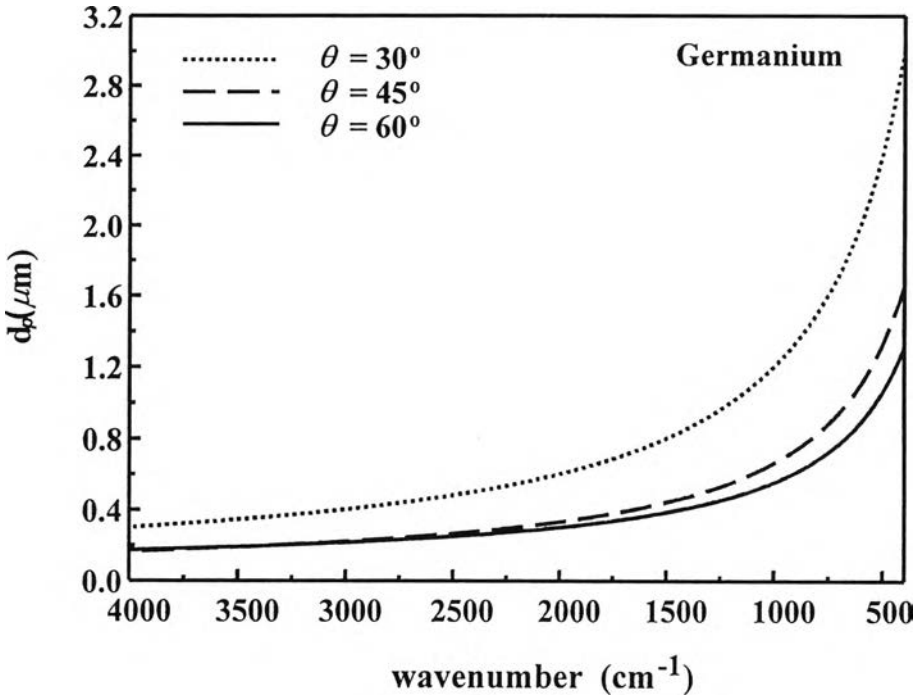

Figure 2.7 Relationship between the penetration depth and wavenumber for Ge crystal (n = 4.0) at different angle of incidence.

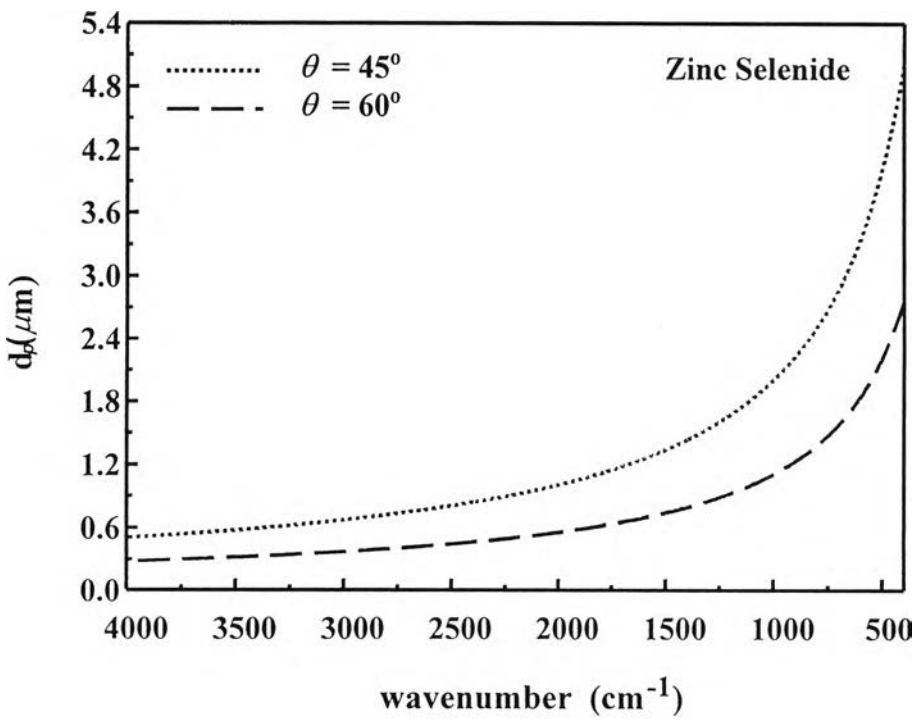

Figure 2.8 Relationship between penetration depth and wavenumber for ZnSe crystal (n = 2.4) at different angle of incidence.

The penetration depth is defined as the depth where the electric field strength decays to 1/e of its value at the interface. Furthermore, the value is also varied as a function of frequency being investigated. The penetration depth at a low frequency is much greater than that at a high frequency.

Under a weakly absorbing condition, the strength and decay characteristic of the MSEF is similar to those of the MSEvF. The MSEF can be accurately estimated from the MSEvF by the following expression:

$$\left\langle E_z^2(\theta,\nu)\right\rangle = \frac{1+R(\theta,\nu)}{2}\left\langle E_z^2(\theta,\nu)\right\rangle_{k=0} \tag{2.11}$$

where $R(\theta,\nu)$ is reflectance and $\left\langle E_z^2(\theta,\nu)\right\rangle$ and $\left\langle E_z^2(\theta,\nu)\right\rangle_{k=0}$, respectively, are the MSEF and MSEvF at depth z.

By substituting Equations 2.10 and 2.11 into Equation 2.6, the absorption in ATR spectroscopy, under a weakly absorbing condition, can be expressed in terms of the MSEvF by the following expression:

$$A(\theta,\nu) = \frac{1+R(\theta,\nu)}{2}\cdot\frac{4\pi\nu\left\langle E_0^2(\theta,\nu)\right\rangle_{k=0}}{n_0\cos\theta}n_1(\nu)k_1(\nu)\int_0^{\infty}e^{-2z/d_p(\theta,\nu)}dz \tag{2.12}$$

By substituting Equation 2.5 into Equation 2.12, the following expression is obtained:

$$2\frac{1-R(\theta,\nu)}{1+R(\theta,\nu)} = \frac{2\pi\nu\left\langle E_0^2(\theta,\nu)\right\rangle_{k=0}n_1(\nu)k_1(\nu)d_p(\theta,\nu)}{n_0\cos\theta_c} \tag{2.13}$$

When absorption is small (i.e., $R(\theta,\nu)$ is close to unity) the above equation is further simplified to:

$$\ln R(\theta, \nu) = \frac{2\pi\nu n_1(\nu)k_1(\nu)d_p(\theta, \nu)\left\langle E_0^2(\theta, \nu)\right\rangle_{k=0}}{n_0 \cos\theta_c} \tag{2.14}$$

$$\mathbf{A}(\theta, \nu) = \frac{2\pi\nu n_1(\nu)k_1(\nu)d_p(\theta, \nu)\left\langle E_0^2(\theta, \nu)\right\rangle_{k=0}}{\ln(10)n_0 \cos\theta} \tag{2.15}$$

where $\mathbf{A}(\theta, \nu)$ is absorbance, which is the value one normally obtained from spectrometer. However, one should not confuse absorptance $A(\theta, \nu)$ given in Equation 5 and absorbance $\mathbf{A}(\theta, \nu)$ given in Equation 2.15 since they are defined based on different criteria.

Equation 2.15 also indicates that spectral intensity is directly related to material characteristic. However, the expression is limited to small absorption since it is derived based on the MSEvF. However, the expression is the most convenient form for expressing quantitative relationship between spectral intensity and material characteristic (i.e., concentration).

2.2.5. Effective Number of Reflections in an IRE

By taking advantage of the interaction between the electric field and the materials in ATR FT-IR spectroscopy, one can gain an insight understanding of the materials. The quantitative nature of an ATR spectrum can be given in terms of experimental parameters (i.e., polarization, angle of incidence and number of reflections) and material characteristics (i.e., refractive index of the IRE and complex refractive index of the material). In order to improve the sensitivity of the technique and the signal-to-noise ratio of the acquired spectrum, a multiple attenuated total reflection (MATR) accessory is normally employed instead of a single reflection accessory. The spectral intensity of a multiple reflection spectrum equals the number of reflections times the intensity of the single reflection spectrum.

In general N is calculated from geometrical dimension of the IRE (see Figure 2.9).

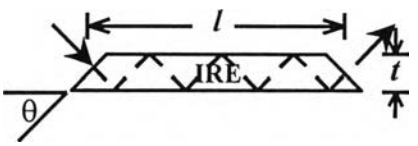

Figure 2.9 Travel path of the beam in an IRE.

The number of reflections for a single pass in the plate is given by [3]:

$$N = (l / t) \cot \theta \tag{2.16}$$

where θ is the angle of incidence, l and t are the length and the thickness of the IRE, respectively. N increases as the plates are made longer and thinner. Because of the practical considerations there are limitations on both l and t. Furthermore, θ must be greater than the critical angle.

Since beam divergence and accessory alignment can introduce a non-uniform beam path in an IRE. The interaction between incident beam and material deviates from that given in Equation 2.15. As a result, the effective number of reflections is not the same as that given in Equation 2.16. However, an effective number of reflections in an IRE can be calculated from ATR and transmission spectra.

ATR spectral intensity depends on both experimental parameters and material characteristics. Transmission spectral intensity at the normal angle of incidence, on the other hand, is a function of the complex refractive index and the thickness of the absorbing medium. However, the information from both techniques enables one to calculate the effective number of reflections in an IRE. An ATR spectral intensity under a weak absorption condition in absorbance units with effective number of reflections N is given by [2, 3, 4-10]:

$$\mathbf{A}_{\bar{p}}(\theta,\nu) = N\frac{2\pi\nu n_1(\nu)k_1(\nu)d_p(\theta,\nu)\left\langle E_{0\bar{p}}^2(\theta,\nu)\right\rangle_{k=0}}{ln(10)n_0\cos\theta}, \qquad (2.17)$$

where $\bar{p}$ indicates the degree of polarization of the incident beam, n_0 is the refractive index of the IRE, $n_1(\nu)$ and $k_1(\nu)$ are the refractive index and the absorption index of the absorbing medium, respectively, $d_p(\theta,\nu)$ is the penetration depth, $\left\langle E_{0\bar{p}}^2(\theta,\nu)\right\rangle_{k=0}$ is the mean square evanescent field (MSEvF) at the IRE/sample interface and N is the *effective* number of reflections in the IRE. The observed spectral intensity in transmission mode is given by [11,12]:

$$\mathbf{A}(\nu) = \frac{1}{\ln(10)}\left\{4\pi h\nu k_1(\nu) + ln\left[\frac{|t_{01}(\nu)|^2|t_{10}(\nu)|^2}{1+R_{01}(\nu)R_{10}(\nu)e^{-8\pi h\nu k_1(\nu)}+2R_{01}^{1/2}(\nu)R_{10}^{1/2}(\nu)\cos\left[\delta_{01}^r(\nu)+\delta_{10}^r(\nu)+4\pi h\nu n_1(\nu)\right]}\right]\right\} \qquad (2.18)$$

where h is the thickness of the absorbing medium, $t_{01}(\nu)$ and $t_{10}(\nu)$ are transmission coefficients, $R_{01}(\nu)$ and $R_{10}(\nu)$ are reflectance, and $\delta_{01}^r(\nu)$ and $\delta_{10}^r(\nu)$ are the phase changes upon reflection at the interfaces between the incident medium (0) and the absorbing medium (1). When the sample has a uniform thickness, there exist sinusoidal fringes in the transmission spectrum due to the multiple reflections at the incident medium/sample interfaces. The term $\cos\left[\delta_{01}^r(\nu)+\delta_{10}^r(\nu)+4\pi h\nu n_1(\nu)\right]$ is responsible for the sinusoidal feature in the transmission spectrum. It is strongly dependent on the product between the refractive index and the thickness since the phase changes upon reflections do not vary considerably over the spectral region. As a result, the sinusoidal feature is mainly an optical effect and is represented by the second term in the right-hand side of Equation 2.18. The fringes can be eliminated by mathematical means. However, they can also be avoided by acquiring a spectrum using a sample with a wedge-shaped or a sample with micro-rough surfaces and/or

collecting spectrum at a near normal angle of incidence [13-17]. The observed spectral intensity without fringes or that after fringe elimination can be used for calculating the effective number of reflections once the thickness of the sample is known.

The effective number of reflections in an IRE can, then, be calculated from observed spectral intensities by the following expression:

$$N = \frac{\mathbf{A}_{\bar{p}}(\theta,\nu)_{\mathrm{ATR}}}{\mathbf{A}(\nu)_{\mathrm{Trans}}} \cdot \frac{2n_0 \cos\theta h}{n_1(\nu) d_p(\theta,\nu) \left\langle E^2_{0\bar{p}}(\theta,\nu) \right\rangle_{k=0}} . \qquad (2.19)$$

Since the above expression is based on a small absorption approximation, it is only applicable for weak absorption bands [4-10].

2.2.6. Optical Contact in ATR Experiment

2.2.6.1. Problem of Sample Contact in ATR Measurement

ATR FT-IR is a surface sensitive technique. Therefore, in order to obtain good ATR spectra, very good contact between the sample and ATR prism or an IRE is required [13]. Liquid samples always have a perfect optical contact with an IRE. Solid samples, on the other hand, rarely have a good contact with an IRE although their surface is obviously flat. This is due to surface irregularity of the samples, imperfect flatness throughout the surface, defect on the surface, and etc. In order to gain a good contact between solid samples and an IRE, pressure has to be applied. If the sample is harder or tougher than the prism material, the pressure applied will leads to rapid deterioration of the prism and still no optical contact is obtained. Unfortunately, the high refractive index materials used for ATR FT-IR are not very strong and the lower wavelength regions require a much better contact [13].

ATR spectral intensity may be increased by working at incident angles approaching the critical angle [13] but this leads to severely distorted spectra. There is, currently, micro ATR accessory used for these solid samples in which the radiation is focused on the specimen's surface [13]. Thus, one can select the best part of the sample surface for analysis, but this is useful only if the sample surface has uniform properties. However, according to the higher sensitivity, multiple reflection ATR can reduces contact quality requirements, but this requires large samples and it stills difficult to observe the weaker bands. Moreover, quantitative analysis by ATR FT-IR spectroscopy requires a perfect optical contact between sample and an IRE.

2.2.6.2. Solution for Sample Contact Problem

It was found that an air gap still presents although pressure is applied to the system. The spectral intensity is drastically decreased by the small air gap because the electric field decays faster in the air than in a sample (see Figure 2.10). According to this, ATR spectral intensity can, then, be enhanced by replacing the air gap with other media with high refractive index. The intermediate layer introduced into the system will act as a contact fluid between the sample and the ATR prism by bringing the two surfaces closer together and changing the decay pattern of the electric field at the interface. This results in increasing spectral intensity and better contact between samples and ATR prism. The intermediate layer used in this research is an organic liquid material of which refractive index is approximately 1.5 and can be easily squeezed out (see Figure 2.11) by an applied pressure. An optical contact or a shorter distance between the IRE and sample is obtained. A better spectral quality will then be observed.

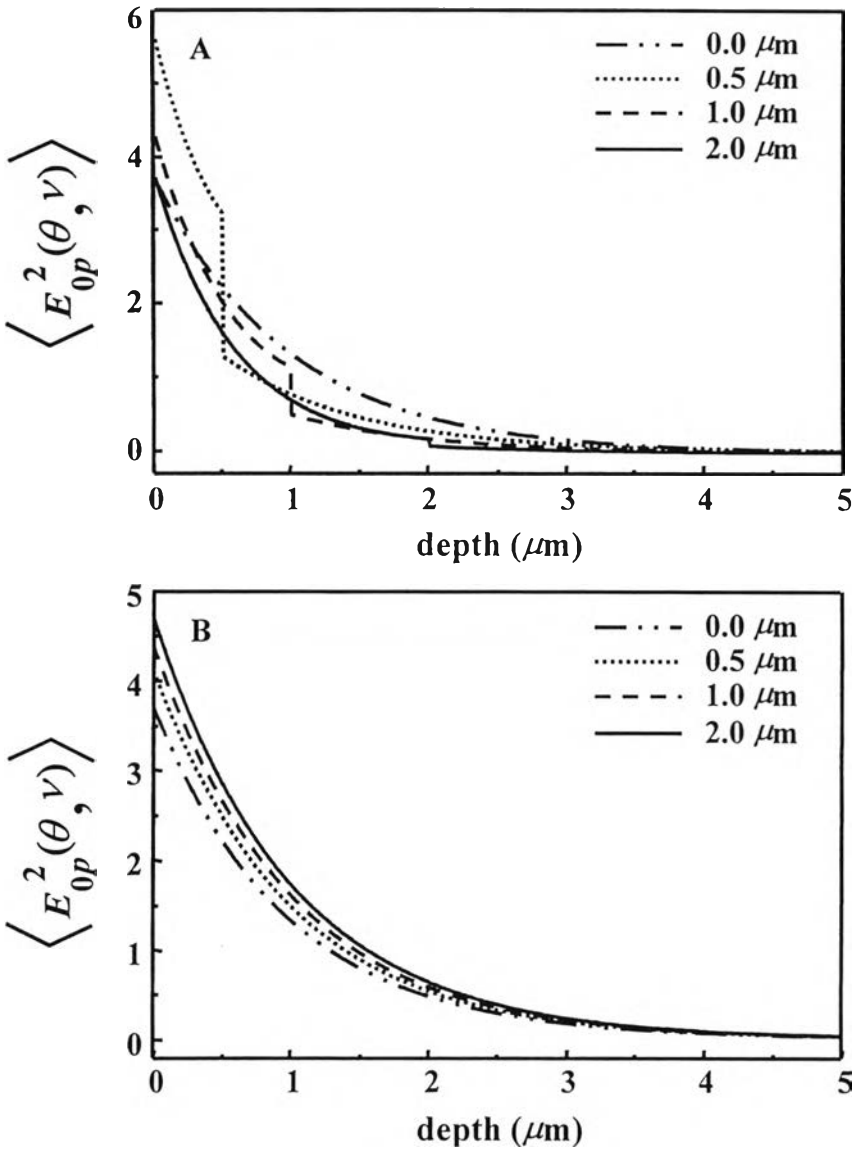

Figure 2.10 Electric field decay pattern: a) system with air gap, and b) system that air gap is replaced with organic liquid at various thickness.

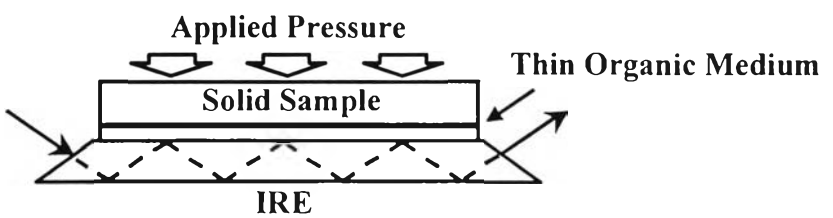

Figure 2.11 Experimental arrangement for the replacement of existent air gap in ATR measurement with an organic medium.

2.2.7. Sampling Depth in ATR FT-IR Spectroscopy

ATR-FTIR spectroscopy has long been recognized as a surface characterization and depth profiling techniques. This is due to the unique characteristic of the mean square electric field (MSEF) under the total internal reflection condition. The MSEF is strongest at the interface between the ATR crystal (or the internal reflection element, IRE) and the optically rarer medium. It decays exponentially as a function of depth from the interface. Therefore, the molecules at the interface contribute mostly in the ATR spectral intensity. Molecules at the distance beyond sampling depth (i.e., the depth where the electric field decays to an insignificant level) do not contribute to the spectral intensity.

2.2.7.1. Information Depth

For an isotropic medium with small absorption coefficient (i.e., most organic materials), the MSEF can be estimated from the mean square evanescent field (MSEvF). The MSEvF can be calculated if refractive index of the material is known. In general, n_F = 1.5 is assumed for most organic materials. Under small absorbing condition, the relationship between spectral intensity and absorption coefficient is linear. Furthermore, the MSEvF at depth z can be simply expressed in terms of the decay constant (i.e., the penetration depth) and its strength at the surface. ATR spectral intensity in *absorbance unit* can be expressed in terms of the MSEvF as:

$$\mathrm{A}_l(\theta,\nu) = \frac{4\pi\nu n_{\mathrm{F}}(\nu)k_{\mathrm{F}}(\nu)\left\langle E_{0l}^2(\theta,\nu)\right\rangle_{k=0}}{ln(10)n_{\mathrm{IRE}}\cos\theta}\int_0^{\infty} e^{-2z/d_p(\theta,\nu)}dz \qquad (2.20)$$

where $\left\langle E_{0l}^2(\theta,\nu)\right\rangle_{k=0}$ is the MSEvF at the surface of the medium, $d_p(\theta,\nu)$ is penetration depth. Since the penetration depth is defined by a distance from the surface where the strength of the MSEvF decays to $1/e$ of that at the surface. As a

result, it does not represent the sampling depth or the final depth where beam interacts with material. It just gives a comparative picture how deep the electric field penetrates into the medium at various angles of incidence and wavenumbers. The electric field is very strong at the IRE/sample interface and exponentially decays as a function of depth, an ATR spectral intensity is then the collective sum of all contributions before the electric field decays to insignificant level. Most contributions come from material near the crystal surface. This is the reason why ATR FT-IR spectroscopy is one of the favorite surface characterization techniques. Ohta and Ishitani [14-16] have pointed out that the smallest significant spectral intensity is given by the value of two times the noise level. By adopting the above criteria, the information depth is then defined by the distance from the surface whose collective sum of the spectral intensity has the same significance as that of the bulk. That means the difference between the bulk spectral intensity and spectral information up to the sampling depth is less than two times the noise level.

$$
\begin{aligned}
2\mathbf{A}_{noise}(\theta,\nu) &= \mathbf{A}_{bulk}(\theta,\nu) - \mathbf{A}_{info}(\theta,\nu) \\
&= \frac{4\pi\nu n_{\mathrm{F}}(\nu)k_{\mathrm{F}}(\nu)\left\langle E_{0l}^{2}(\theta,\nu)\right\rangle_{k=0}}{\ln(10)n_{\mathrm{IRE}}\cos\theta}\int_{z_{info}}^{\infty} e^{-2z/d_p(\theta,\nu)}dz \\
&= \frac{2\pi\nu n_{\mathrm{F}}(\nu)k_{\mathrm{F}}(\nu)\left\langle E_{0l}^{2}(\theta,\nu)\right\rangle_{k=0} d_p(\theta,\nu)}{ln(10)n_{\mathrm{IRE}}\,cos\theta} e^{-2z_{info}/d_p(\theta,\nu)} \\
&= \mathbf{A}_{bulk}(\theta,\nu)e^{-2z_{info}/d_p(\theta,\nu)} \\
z_{info} &= \frac{d_{p(\theta,\nu)}}{2}\ln\left[\frac{\mathbf{A}_{bulk}(\theta,\nu)}{2\mathbf{A}_{noise}(\theta,\nu)}\right]
\end{aligned}
\tag{2.21}
$$

where $\mathbf{A}_{noise}(\theta,\nu)$ is the noise level which can be obtained experimentally. The above equation indicates that the sampling depth is not only depends on experimental conditions and material characteristics but also instrumental setup (i.e., noise level). Although the MSEvF decays with a definite pattern at a given wavenumber, the information depth, z_{info}, of a stronger absorption band is greater than that of a weak absorption one. The value of the information depth has nothing to do with decay

characteristic of the MSEvF but the distance from the interface where spectral information can be obtained with respect to noise level. As a result, material beyond information depth has insignificant contribution to the observed spectral intensity.

2.2.7.2. The Verification of the Proposed Equation

Due to specific characteristic of the electric field at the interface of two media under total internal reflection condition that the electric field decays exponentially as a function of the depth into the rarer medium, the proposed equation (i.e., Equation 2.21) can, then, be experimentally verified. By varying the thickness of an intermediate layer (i.e., organic liquid) between substrate (i.e., sample) and the IRE in three-phase system measurement, different spectral intensity of both organic liquid and substrate will be obtained. The thickness of organic liquid film, which varied by an applied pressure can be determined once the spectral intensity of the three-phase system spectrum is known from the following expression [4]:

$$\mathbf{A}_{3\,\text{Phase}}(\theta,\nu) = (1 - e^{-2h\,/\,d_p(\theta,\nu)})\mathbf{A}_{\text{Film}}(\theta,\nu) + e^{-2h\,/\,d_p(\theta,\nu)}\mathbf{A}_{\text{Substrate}}(\theta,\nu) \tag{2.22}$$

where $\mathbf{A}_{3\,\text{Phase}}(\theta,\nu)$ is spectral intensity in absorbance unit of a three-phase system spectrum and $\mathbf{A}_{\text{Film}}(\theta,\nu)$ and $\mathbf{A}_{\text{Substrate}}(\theta,\nu)$ are spectral intensity in absorbance unit of bulk materials, respectively.

According to the decay characteristic of the electric field under total internal reflection condition at different wavenumber, as can be seen in Figures 2.7 and 2.8, the spectral intensity of materials in the region of low wavenumber will be more sensitive to the change in the thickness of organic liquid film than the region of high wavenumber. Therefore, the thickness of organic liquid film calculated from experimental result via Equation 2.22 can be used to verify the sampling depth or Z_{info} at the high wavenumber in the same spectrum by comparing the thickness of the liquid film calculated from the region of low wavenumber with the sampling

depth calculated from the region of high wavenumber in each same spectrum. The thickness of the liquid film at which the change in spectral intensity in the region of high wavenumber in the same spectrum can be observed should be similar to the sampling depth calculated at that particular wavenumber.